

Scaling behaviour at the $N_t = 6$ chiral phase transition for
 2-flavour lattice QCD with massless staggered quarks, and an
 irrelevant 4-fermion interaction.

J. B. Kogut

Dept. of Physics, University of Illinois, 1110 West Green Street, Urbana, IL 61801-3080, USA

D. K. Sinclair

HEP Division, Argonne National Laboratory, 9700 South Cass Avenue, Argonne, IL 60439, USA

Abstract

We have simulated lattice QCD with 2 flavours of massless staggered quarks. An irrelevant chiral 4-fermion interaction was added to the standard quark action to allow us to simulate at zero quark mass. Thermodynamics was studied on lattices of temporal extent 6. Clear evidence for a second order chiral transition was observed and the critical exponents ν , β , and γ were measured. These exponents did not agree with those expected by standard universality arguments. They were, however, consistent with tricritical behaviour. The χ and χ screening masses were measured and showed clear evidence for chiral symmetry restoration at this transition.

12.38 Mh, 12.38 Gc, 11.15 Ha

I. INTRODUCTION

In standard methods for simulating lattice QCD, [1] the Dirac operator (matrix) becomes singular in the limit of zero quark mass. Since these methods require inversion of the Dirac operator they therefore fail for zero quark mass. The iterative methods for performing these inversions become progressively less efficient, requiring a number of iterations which diverges as this zero mass limit is approached. This means that, even at the mass of the physical u and d quarks, simulations on modest size lattices become prohibitively expensive in computer time, and most simulations are performed with unphysically large light-quark masses.

QCD with 2 light quark flavours is expected to undergo a second order chiral transition at finite temperature, only in the zero mass limit. It would thus be very helpful to be able to simulate in this limit in order to extract detailed information about this transition such as critical exponents and the equation of state in the neighbourhood of this transition. Here we note a second difficulty with the standard action. In the zero mass limit on a finite lattice, the chiral condensate which we need to use as an order parameter vanishes on a configuration by configuration basis, which restricts how small a mass we can use on a given lattice size. This contrasts with the behaviour of most lattice spin models, where the magnetization (the order parameter for this class of models) has a finite value close to the infinite volume limit (for large enough lattices), even for zero magnetic field, for each configuration. The way in which the magnetization averages to zero over the ensemble of configurations, which it must for zero applied magnetic field, is that the direction of magnetization changes from configuration to configuration to enforce this. On a large enough lattice, a reasonable approximation to the spontaneous magnetization is obtained by averaging the magnitude of the magnetization (or its square) over the ensemble.

To enable simulations at zero quark mass, we have modified the standard staggered quark action by the addition of an irrelevant 4-fermion term which preserves the symmetries

of the lattice action [2]. Such a term will not affect the continuum limit of the theory. It does, however, serve to render the Dirac operator non-singular at zero quark mass. In the hadronic phase, where the chiral symmetry is spontaneously broken, this is easy to understand. The chiral condensate provides an effective mass to the quarks through the 4-fermion coupling. Even where the 4-fermion coupling is small, as it must be close to the continuum limit, this "constituent" quark mass is large enough to keep the number of iterations required to invert the Dirac operator manageable. With the standard staggered fermion action, the finite time extent of the lattice keeps the Dirac operator from becoming singular in the plasma phase. It does, however, become nearly singular for topologically non-trivial gauge configurations due to the lattice remnant of the Atiyah-Singer index theorem [3]. For our modified action, the conservation of the axial quark-number current is explicitly broken by the 4-fermion interaction, thus avoiding this consequence of the index theorem. This keeps the number of iterations required to invert the Dirac operator manageable in the plasma phase.

Although early attempts to extract critical exponents from staggered-quark lattice QCD appeared promising [4], later attempts showed significant deviations from the $O(4)$ or $O(2)$ exponents expected from universality arguments. [5,6] Attempts to fit scaling with $\beta = 6/g^2$ and quark mass m to the scaling functions of the $O(4)$ and $O(2)$ 3-dimensional spin models [7] failed for lattices of temporal extent $N_t = 4$ [8,9]. While the situation appeared better for $N_t > 6$ ($N_t = 6$ was somewhat ambiguous) insufficient "data" existed to make this conclusive.

Our earlier simulations with our new action on $N_t = 4$ lattices at $m = 0$ indicated that the transition was probably first order [2]. Ongoing simulations on an $N_t = 4$ lattice with a smaller 4-fermion coupling indicate that the chiral transition is either a first order or a very narrow second order transition. The results of our simulations on $12^3 \times 6$ and $18^3 \times 6$ lattices summarized in an earlier letter [10] and presented in detail in this paper, indicate that the $N_t = 6$ transition is second order, but with the critical exponents of the 3-dimensional tricritical point, rather than those of the $O(4)$ or $O(2)$ spin models. We were

able to arrive at this conclusion because we were able to study the scaling of the chiral condensate with β at $m = 0$ and thus extract the critical exponent ν_{mag} .

Section 2 describes our modified action. In section 3 we discuss the critical phenomena relevant to these simulations. We describe our simulations and results in section 4. In section 5 we discuss our fits to critical scaling. Section 6 gives our conclusions.

II. LATTICE QCD WITH CHIRAL 4-FERMION INTERACTIONS.

We have modified our staggered quark lattice QCD action by the addition of an irrelevant chiral 4-fermion interaction. In the continuum the Euclidean Lagrangian density of this theory is

$$L = \frac{1}{4} \bar{\psi} \not{D} \psi + (\bar{\psi} + m) \frac{1}{6N_f} [(\bar{\psi} \psi)^2 + (\bar{\psi} \gamma_5 \psi)^2]: \quad (1)$$

Lattice field theories incorporating fermions interacting both through gauge fields and through quartic self-interactions have been studied before | see for example [11], [12], [13-15] | with promising preliminary results.

Equation 1 can be rendered quadratic in the fermion fields by the standard trick of introducing (non-dynamical) auxiliary fields and in terms of which this Lagrangian density becomes

$$L = \frac{1}{4} \bar{\psi} \not{D} \psi + (\bar{\psi} + i \gamma_5 \psi + m) \frac{3N_f}{2} (\sigma^2 + \tau^2) \quad (2)$$

The molecular dynamics Lagrangian for a particular staggered fermion lattice transcription of this theory in which σ is identified with τ , the flavour equivalent of τ , is

$$L = \sum_x \left[\frac{1}{3} \text{Re}(\text{Tr}_2 UUUU) \right] + \frac{N_f}{8} \sum_s \gamma_A \gamma_A - \sum_s \frac{1}{8} N_f (\sigma^2 + \tau^2) + \frac{1}{2} \sum_x \left(\tau^2 + \frac{2}{8} + \tau_1 \tau_1 + \tau_2 \tau_2 + \tau_3 \tau_3 \right) + \frac{1}{2} \sum_s (\sigma^2 + \tau^2) \quad (3)$$

where

$$A = \not{D} + m + \frac{1}{16} \sum_i \chi_i (\psi_{i+1} \psi_i) \quad (4)$$

with i running over the 16 sites on the dual lattice neighbouring the site on the normal lattice, $\chi_i = (1)^{x+y+z+t}$ and \not{D} the usual gauge-covariant "d-slash" for the staggered quarks. The factor $\frac{N_f}{8}$ in front of the pseudo-fermion kinetic term is appropriate for the hybrid molecular dynamics algorithm with "noisy" fermions, where A_i are chosen from a complex gaussian distribution with width 1. The "dots" represent derivatives with respect to molecular dynamics "time" as distinct from normal time. We note that $\det A = 3^{-2}$. Although the determinant of A does not appear to be real, it becomes so in the continuum limit. Without the gauge fields, this theory reverts to the one studied in [14], with $3N_f$ flavours.

The advantage of this choice of the chiral 4-fermion interaction is that it preserves the axial $U(1)$ chiral symmetry of the normal staggered quark lattice QCD action generated by $\psi_5 \psi_5$ at $m = 0$. This means that, when chiral symmetry is spontaneously broken, the pion associated with $\psi_5 \psi_5$ will be a true Goldstone boson and will be massless at $m = 0$, even for finite lattice spacing. Under this exact chiral symmetry the fields transform as

$$\psi_{(n)} \rightarrow e^{i\frac{1}{2} \theta} \psi_{(n)} \quad (5)$$

$$\psi_{(n)+i} \rightarrow e^{i\theta} [\psi_{(n)+i} \psi_{(n)}] \quad (6)$$

from which we find that

$$A_{(n)} \rightarrow e^{i\frac{1}{2} \theta} A_{(n)} \quad (7)$$

$$\psi_{(n)+i} \psi_{(n)} \rightarrow e^{i\theta} [\psi_{(n)+i} \psi_{(n)}]; \quad (8)$$

when $m = 0$. Hence, for massless quarks the above Lagrangian has an exact $U(1)$ axial flavour symmetry, the same remnant of continuum chiral flavour symmetry as the standard staggered lattice Lagrangian.

III. CRITICAL BEHAVIOUR OF THE CHIRAL TRANSITION IN LATTICE

QCD

Near a critical point, the order parameters of the theory in question scale as powers of the parameters in the theory. Since chiral symmetry is restored at the finite temperature transition from hadronic matter to a quark-gluon plasma, the appropriate order parameter is the chiral condensate, $\langle \bar{\psi} \psi \rangle$. The equation of state describing the scaling of this order parameter close to the critical point is of the form [16]

$$\langle \bar{\psi} \psi \rangle = h^{1/\nu} f_{\text{QCD}}(th^{1/\nu - m_{\text{ag}}}) \quad (9)$$

where $h = m - T$ and $t = (T - T_c)/T_c$. f_{QCD} is called the scaling function. This also serves to define 2 of the critical exponents, ν and β . Since $\langle \bar{\psi} \psi \rangle$ is non-zero for $h = 0$, $t < 0$ equation 9 requires

$$f_{\text{QCD}}(x) = C(x); \quad x \neq 1; \quad (10)$$

so that

$$\langle \bar{\psi} \psi \rangle = C(t)^{m_{\text{ag}}}; \quad t < 0; \quad (11)$$

At $t = 0$,

$$\langle \bar{\psi} \psi \rangle = D h^{1/\nu}; \quad D = f_{\text{QCD}}(0); \quad (12)$$

Clearly, since $\langle \bar{\psi} \psi \rangle = h^{1/\nu}$, similar scaling relations exist for $\langle \bar{\psi} \psi \rangle$. In addition, at $h = 0$, the screening mass vanishes as

$$m = A |t|^\beta; \quad (13)$$

since the correlation length of the system diverges as $1/m$. Finally we need to consider the scaling relations for the susceptibilities which measure the fluctuations in the

order parameter(s). For reasons which will be explained later, we consider the scaling of the susceptibility χ , rather than that for χ_i , with t . Near $t = 0$, χ diverges as

$$\chi = V^{-1} \langle \langle \sum_i \langle \chi_i^2 \rangle \rangle \rangle = c |t|^{-\nu_{\text{mag}}} \quad (14)$$

Here the inner angle brackets represent averages over the lattice for a single configuration while the outer angle brackets represent averages over the ensemble of configurations.

Let us briefly give the arguments which indicate the expected universality class for this transition. First one notes that the Matsubara frequencies for bosonic excitations are $2n\pi T$, while those for fermionic excitations are $(2n+1)\pi T$ [17]. The expectation that only low lying excitations contribute to critical phenomena leads one to the expectation that, at high T , only the lowest bosonic excitation $n = 0$ contributes and the fermions decouple. Since this lowest bosonic mode is independent of time, this leads to an effective 3-dimensional theory (dimensional reduction) [18]. Since the masses of the $(\psi; \bar{\psi})$ chiral multiplet vanish at the chiral transition, these excitations alone should determine the critical scaling at this transition. The effective field theories describing the interactions of the $(\psi; \bar{\psi})$ multiplet are 3-dimensional $O(4)$ sigma models. Thus 2-flavour QCD should lie in the universality class of the $O(4)$ sigma model in 3-dimensions [18], with critical exponents $\nu_{\text{mag}} = 0.384(5)$, $\beta = 4.85(2)$, $\gamma = 0.749(4)$ and $\nu_{\text{mag}} = 1.471(6)$ [19]. Of course, lattice QCD with staggered quarks has only one Goldstone pion, and this symmetry is reduced to $O(2)$. Thus if the lattice is coarse enough that this symmetry breaking is relevant, 2-flavour QCD should lie in the universality class of the $O(2)$ sigma model in 3-dimensions, with critical exponents $\nu_{\text{mag}} = 0.35(1)$, $\beta = 4.81(1)$, $\gamma = 0.679(3)$ and $\nu_{\text{mag}} = 1.328(6)$ [19].

Of course, other possibilities exist. First the transition could be first order, which appears to be the case at $N_t = 4$ with our first choice of 4-fermi coupling [2]. Once the lattice spacing is large enough that lattice artifacts can affect the transition, more symmetry breaking and symmetry conserving operators come into play giving a more complex transition. The simplest of these is the tricritical point. The sigma models which give the

universal critical points discussed in the previous paragraph lie in the universality class of the polynomial sigma models which are quartic in the fields. Tricritical behaviour occurs in sigma models which are sixth order in the fields [20]. This means that there is a second symmetry preserving parameter or temperature and a second symmetry breaking parameter or magnetic field. Since 3 is the upper critical dimension for such sigma models, the critical exponents are given by a mean field analysis. Thus $\nu_{\text{mag}} = \frac{1}{4}; \frac{1}{2}$, the $\beta = 5; 3$, $\gamma = \frac{1}{2}$, $\delta = 1; \frac{1}{2}$. The 2 values of ν_{mag} , and β describe the scalings when the 2 magnetic fields are varied independently. Even more values are possible when we take into account the second temperature. A tricritical point occurs where a line of first order phase transitions continues as a line of second order phase transitions or in general where there are 2 competing phase transitions.

IV. FINITE TEMPERATURE SIMULATIONS AND RESULTS FOR $N_T = 6$.

Our $N_t = 4$ simulations at $\beta = 10$ which showed evidence for a first order transition were reported in an earlier paper [2]. Here we present the details of our simulations on $12^3 \times 6$ and $18^3 \times 6$ lattices. A brief summary of these results were given in a letter [10]. Our $12^3 \times 6$ simulations were performed at $\beta = 10$ and $\beta = 20$ while our $18^3 \times 6$ simulations were done at $\beta = 20$.

We shall first discuss our results for zero mass quarks. Here, without the benefit of the symmetry breaking interaction (quark mass term), the direction of symmetry breaking changes over the run so that $\langle \bar{\psi}_i \psi_i \rangle$ and $\langle \bar{\psi}_i \psi_i \rangle$ and the corresponding chiral condensates $\langle \bar{\psi}_i \psi_i \rangle$ and $\langle \bar{\psi}_5 \psi_5 \rangle$ (where the $\bar{\psi}_i$ is averaging only over the lattice, not the ensemble) average to zero over the ensemble. It is in this way that the absence of spontaneous breaking of this continuous symmetry on a finite lattice is enforced. Note that this contrasts with the standard lattice formulation, where if we could simulate at zero quark mass, the chiral condensates would vanish on a configuration by configuration basis, and there would be no

way to predict the infinite lattice results. In our case, we can estimate the infinite lattice results by averaging the magnitudes $\frac{1}{V} \sum_i \langle h_i^2 \rangle$ and $\frac{1}{V} \sum_i \langle h_{55}^2 \rangle$, introducing an error which is of order $1/\sqrt{V}$ on a lattice of 4-volume V .

The simulations of equation 3 were performed using the hybrid molecular-dynamics algorithm with "noisy" fermions, allowing us to tune the number of flavours to 2. The simulations on the $18^3 \times 6$ lattice were performed at 14 values from 5.39 to 5.45. The behaviour of the chiral condensate and Wilson line (Polyakov loop) are given in figure 1. The

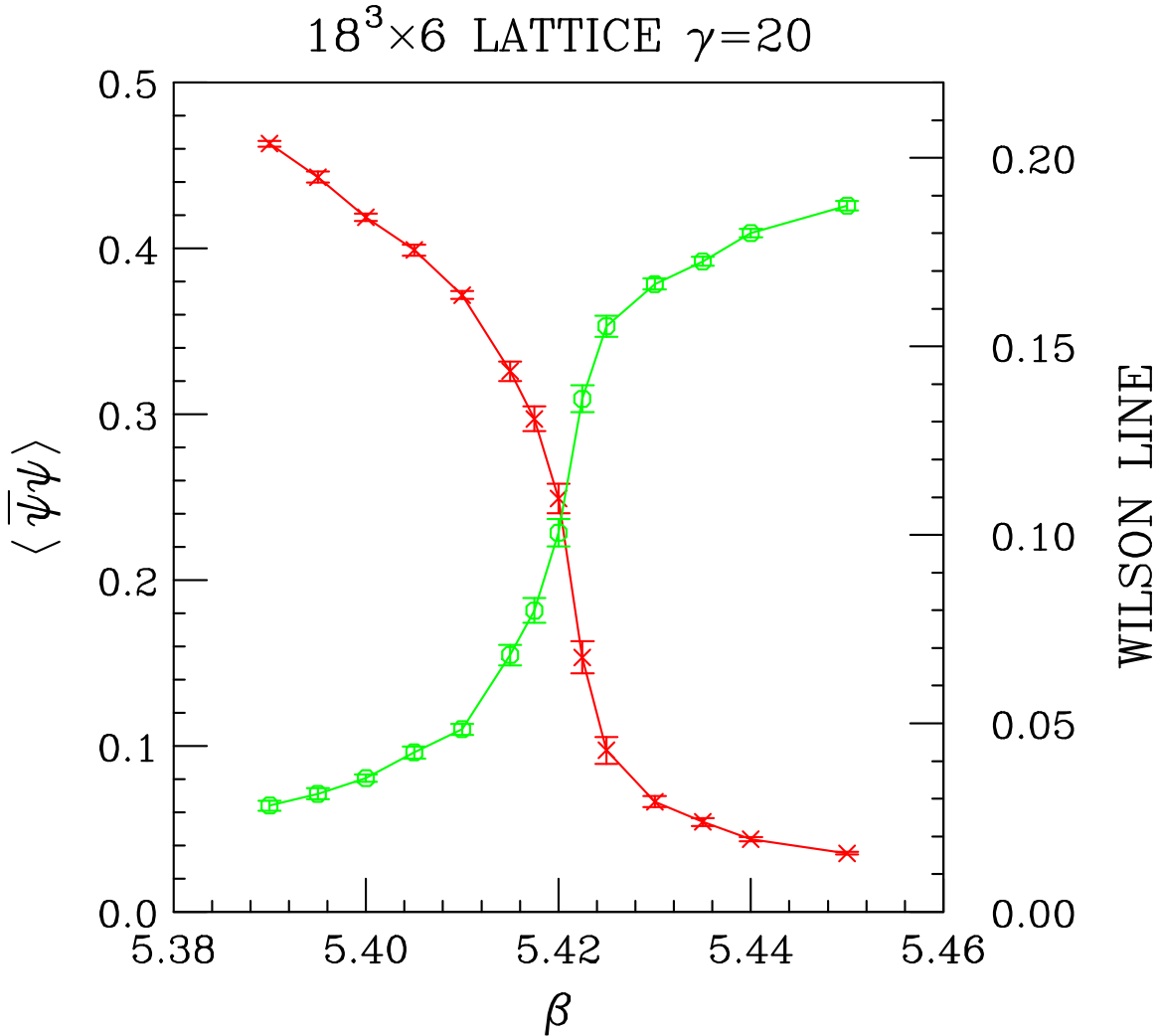


FIG. 1. $\langle \bar{\psi}\psi \rangle$ and Wilson line as functions of β on an $18^3 \times 6$ lattice at $\gamma = 20$.

values of the chiral condensate and $\langle h_i \rangle$ (actually the magnitudes defined above) as well as the length of each run in molecular-dynamics time units are given in table I. (Note this "time"

is twice that of equation 3 for consistency with that used by the HEM CGC and HTM CGC collaborations.) Let us make several observations with regard to these measurements. The

	h_i	h_i	Time'
5.3900	0.4630 (18)	0.02543 (10)	5000
5.3950	0.4430 (32)	0.02454 (16)	5000
5.4000	0.4186 (23)	0.02337 (11)	10000
5.4050	0.3990 (33)	0.02244 (17)	10000
5.4100	0.3719 (23)	0.02109 (12)	20000
5.4150	0.3259 (58)	0.01880 (30)	40000
5.4175	0.2973 (74)	0.01734 (40)	50000
5.4200	0.2491 (89)	0.01479 (48)	50000
5.4225	0.1535 (96)	0.00957 (53)	50000
5.4250	0.0973 (81)	0.00649 (45)	20000
5.4300	0.0664 (33)	0.00479 (18)	20000
5.4350	0.0542 (25)	0.00414 (13)	10000
5.4400	0.0439 (12)	0.00364 (7)	10000
5.4500	0.0353 (8)	0.00326 (5)	5000

TABLE I. h_i , h_i and run length versus β_c on an $18^3 \times 6$ lattice at $\beta = 20$.

First is that the phase transition occurs at $5.4225 < \beta_c < 5.4250$. The second is that due to fluctuations both h_i and h_i are appreciable in the plasma phase. The third observation is that there are considerable deviations from the expected relation

$$h_i = h_i \quad (15)$$

Part of this is attributable to these quantities having different $1 = \frac{P}{V}$ fluctuations, which is why the deviations become worse as β_c increases. The second is $O(dt^2)$ (and higher) errors which are quite large at this β_c for the $dt = 0.05$ we use. These errors affect h_i much more than h_i and could presumably have been reduced by scaling the 'kinetic' term in

equation 3 by a scale factor greater than 1, thus slowing the time evolution of χ and ϕ . For this reason we perform our critical scaling analyses on h_{χ} rather than h_{ϕ} . These assertions have been quantified for our $N_t = 4$, $\beta = 20$ simulations and are presented in table II, which suggests that both effects are coming into play. In fact, assuming a $1 = \frac{P}{V}$ dependence for h_{χ} and h_{ϕ} would give 0.7062 and 0.03760 for their infinite volume limits on an $N_t = 4$ lattice at $\beta = 5.27$ and $dt = 0.05$, giving a ratio of 19.22. If, in addition, we assumed the coefficient of $1 = \frac{P}{V}$ to be the same at $dt = 0.0125$ we would find $h_{\chi} = 0.7526$ and $h_{\phi} = 0.03760$ and the ratio 20.02 at this dt . Assuming the finite dt error is $O(dt^2)$ leads to an estimate of 20.07 for the infinite volume zero dt limit which is consistent with the correct value of 20. Our results for the $12^3 \times 6$ runs at $\beta = 20$ are

$8^3 \times 4$ lattice			
dt	h_{χ}	h_{ϕ}	$h_{\chi} = h_{\phi}$
0.0125	0.7853 (42)	0.04051 (22)	19.38 (4)
0.0250	0.7898 (42)	0.04114 (21)	19.19 (4)
0.0500	0.7929 (38)	0.04246 (19)	18.68 (4)
0.1000	0.8175 (30)	0.04715 (16)	17.34 (3)
$12^2 \times 24 \times 4$ lattice			
dt	h_{χ}	h_{ϕ}	$h_{\chi} = h_{\phi}$
0.0500	0.7728 (27)	0.04067 (14)	19.00 (3)

TABLE II. dt and volume dependence of h_{χ} , h_{ϕ} and their ratios at $\beta = 5.27$.

presented in table III, while those for our $12^3 \times 6$ runs at $\beta = 10$ are given in table IV.

The smoothness of the transition with no hints of metastability suggests a second order transition. Further evidence for this is the fluctuations with long time constants which are obvious from time histories of the chiral condensate close to the transition for the $18^3 \times 6$ lattice at $\beta = 20$, shown in figures 2, 3.

On the largest ($18^3 \times 6$) lattice, we have measured the screening propagators for the

	h_i	Time'
5.39000	0.478 (3)	3500
5.39500	0.444 (7)	2000
5.40000	0.427 (3)	3500
5.40500	0.420 (3)	5000
5.41000	0.376 (4)	6500
5.41500	0.339 (5)	7500
5.41750	0.299 (6)	40000
5.42000	0.261 (4)	50000
5.42125	0.245 (7)	30000
5.42250	0.210 (5)	40000
5.42500	0.200 (5)	45000
5.43000	0.137 (6)	75000

TABLE III. h_i and run length versus β on an $12^3 \times 6$ lattice at $\mu = 20$.

and ψ elds, i.e. the ψ and ψ propagators for spatial separations. For this we use the ψ and ψ auxiliary elds. This has the advantage over using fermion bilinears with the same quantum numbers in that it automatically includes the disconnected contributions to both these elds. Below the transition, we define our ψ eld by globally rotating our ψ elds so that $h_i = 0$ on each configuration. This is the best we can do since the direction of symmetry breaking rotates from configuration to configuration. Our zero momentum and screening propagators are then defined by

$$S(Z) = \frac{1}{V} \sum_z \sum_{xyt} \sum_{x^0 y^0 t^0} \langle \psi(x;y;z;t) \psi(x^0;y^0;z+Z;t^0) \rangle^5 N_x N_y N_t h_i^2 \quad (16)$$

$$P(Z) = \frac{1}{V} \sum_z \sum_{xyt} \langle \psi(x;y;z;t) \psi(x^0;y^0;z+Z;t^0) \rangle^5 \quad (17)$$

We note that $P(Z)$, so defined, obeys

$$\sum_z P(Z) = 0 \quad (18)$$

	h_i	Time'
5.4	0.648 (5)	1500
5.41	0.616 (4)	1500
5.42	0.585 (5)	1500
5.43	0.539 (2)	10000
5.44	0.496 (2)	10000
5.45	0.436 (2)	35000
5.455	0.389 (2)	70000
5.46	0.330 (3)	45000
5.46125	0.302 (3)	60000
5.4625	0.267 (3)	60000
5.46375	0.234 (4)	35000

TABLE IV. h_i and run length versus β on an $12^3 \times 6$ lattice at $\beta = 10$.

Hence we should fit $P(Z)$ to the form

$$P(Z) \sim A [\exp(-Zm) + \exp(-(N_z - Z)m)] + \text{constant} \quad (19)$$

Such fits in this low temperature domain yield values of m in the range $0.1 < m < 0.3$. However, good fits are also obtained by fitting to a zero mass pion propagator. The reason for this is clear. Over the relatively small range we can fit these propagators on an $N_z = 18$ lattice, equation 19 is well approximated by the parabola

$$P(Z) \sim A m^2 (Z - N_z/2)^2 + [2A \exp(-m N_z/2) + \text{constant}] \quad (20)$$

which is the form of the zero mass propagator. Hence when we graph the mass, we will use our knowledge that it must vanish when the chiral symmetry is broken to set it to zero below the transition. We fit $S(Z)$ to the form

$$S(Z) \sim B [\exp(-Zm) + \exp(-(N_z - Z)m)] + C [\exp(-Zm_2) + \exp(-(N_z - Z)m_2)] \quad (21)$$

$18^3 \times 6$ LATTICE $\beta=5.42$ $\gamma=20$

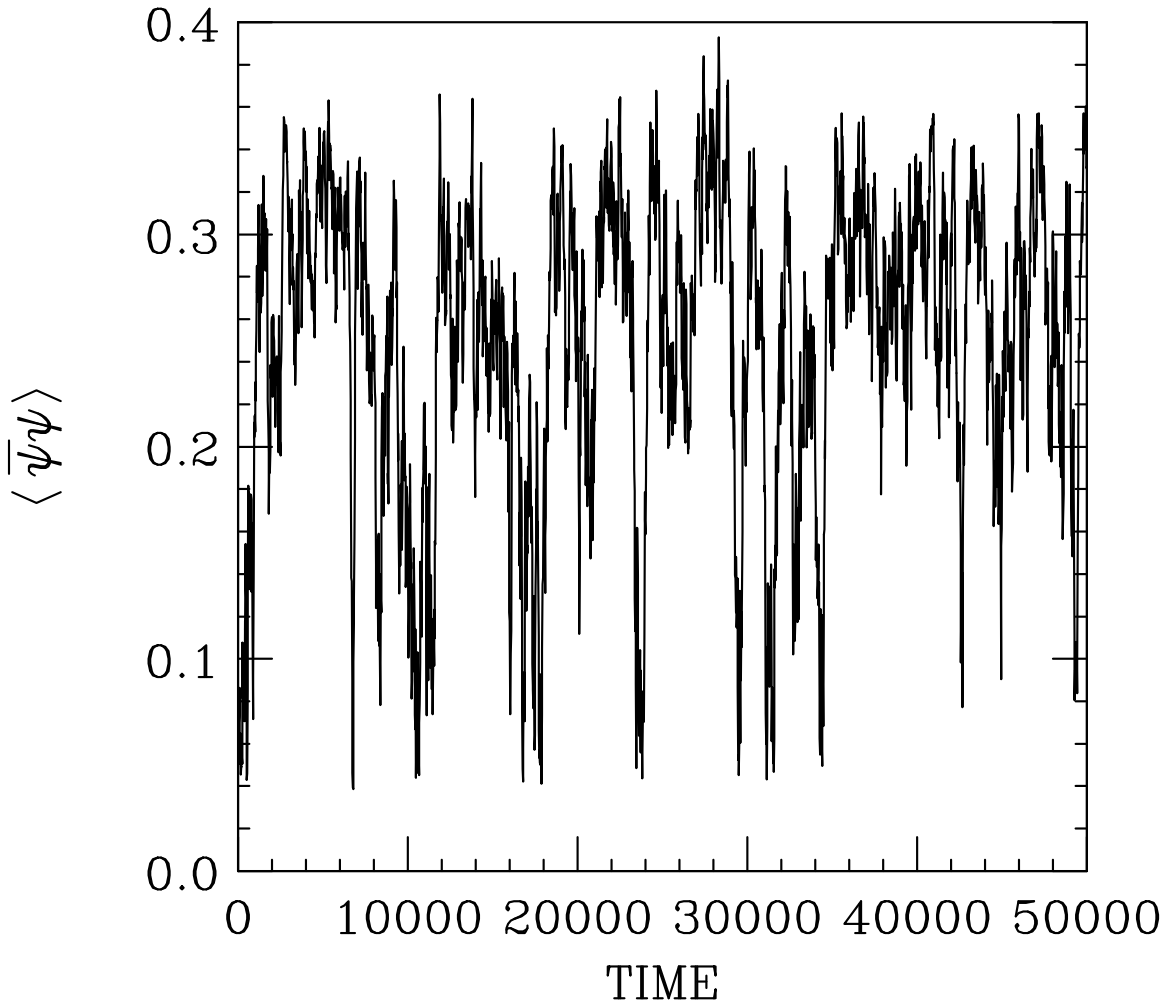


FIG. 2. Time history of $\langle \bar{\psi}\psi \rangle$ at $\beta=5.42$.

and a similar t with $C = 0$, and choose the t with the best signal in this low temperature phase. In the high temperature phase the restoration of chiral symmetry means that we can no longer distinguish $\langle \bar{\psi}\psi \rangle$ and $\langle \bar{\psi}\psi \rangle$. The best propagator to use in this plasma phase is $P_S(Z)$ defined as

$$P_S(Z) = P(Z) + S(Z) \quad (22)$$

Note here we do not have to rotate our fields. We then fit to the form

$$P_S(Z) \sim A [\exp(-Zm) + \exp(-(N_Z - Z)m)]: \quad (23)$$

$18^3 \times 6$ LATTICE $\beta=5.4225$ $\gamma=20$

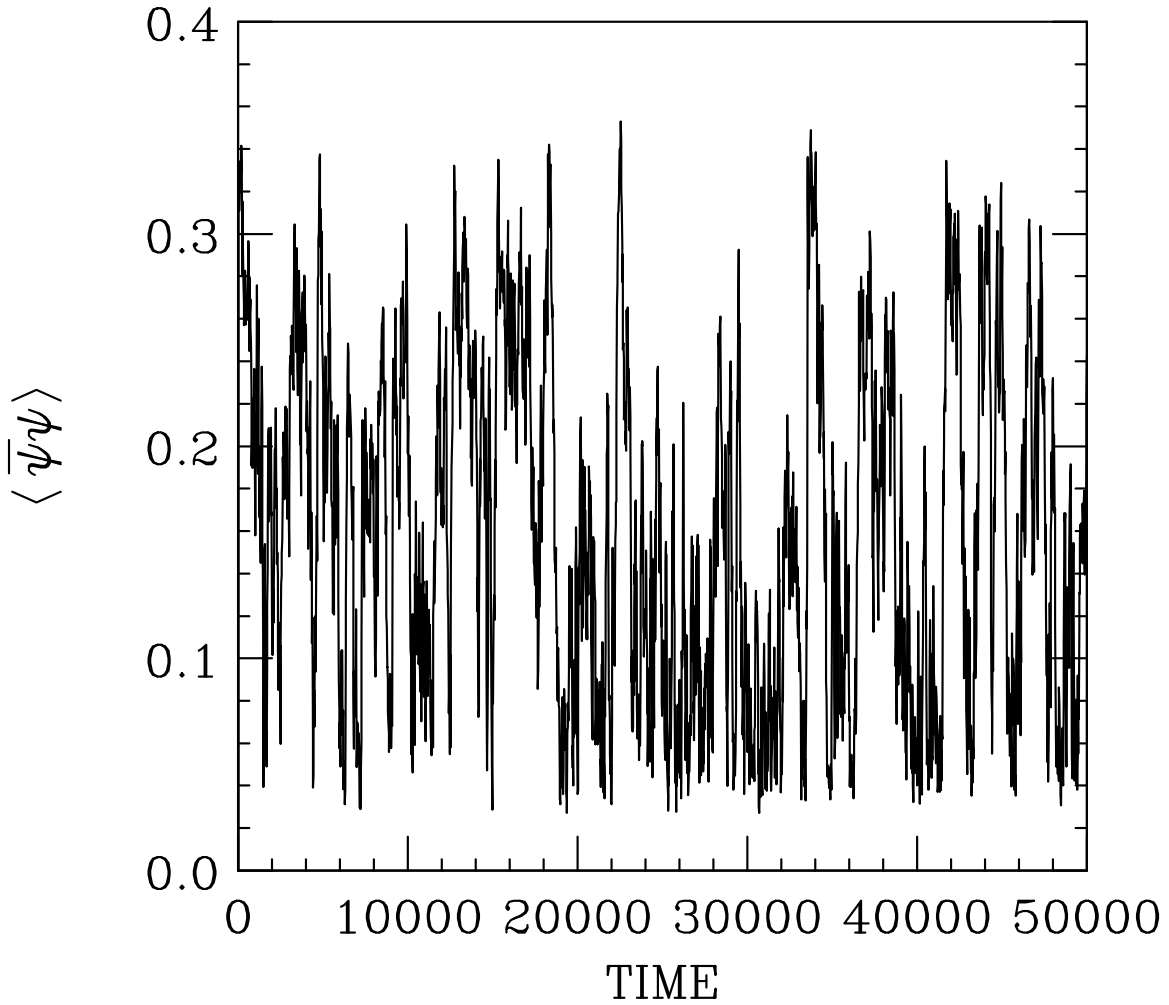


FIG. 3. Time history of $\langle \bar{\psi}\psi \rangle$ at $\beta = 5.4225$.

The screening masses obtained in this way are plotted in figure 4. We note the mass approaches zero as we approach the transition from the low temperature side. The combined $\langle \bar{\psi}\psi \rangle$ mass rises from zero as we enter the plasma phase. However, even at the highest T we consider, it is still far below the expected infinite temperature limit of $2 T = 3$.

In addition, we measured contributions to the energy density, pressure and entropy density. Extraction of energy density or pressure would require measurements at the same values at zero temperature. Hence we concentrate on the entropy density which can be

18³×6 Lattice $\gamma=20$

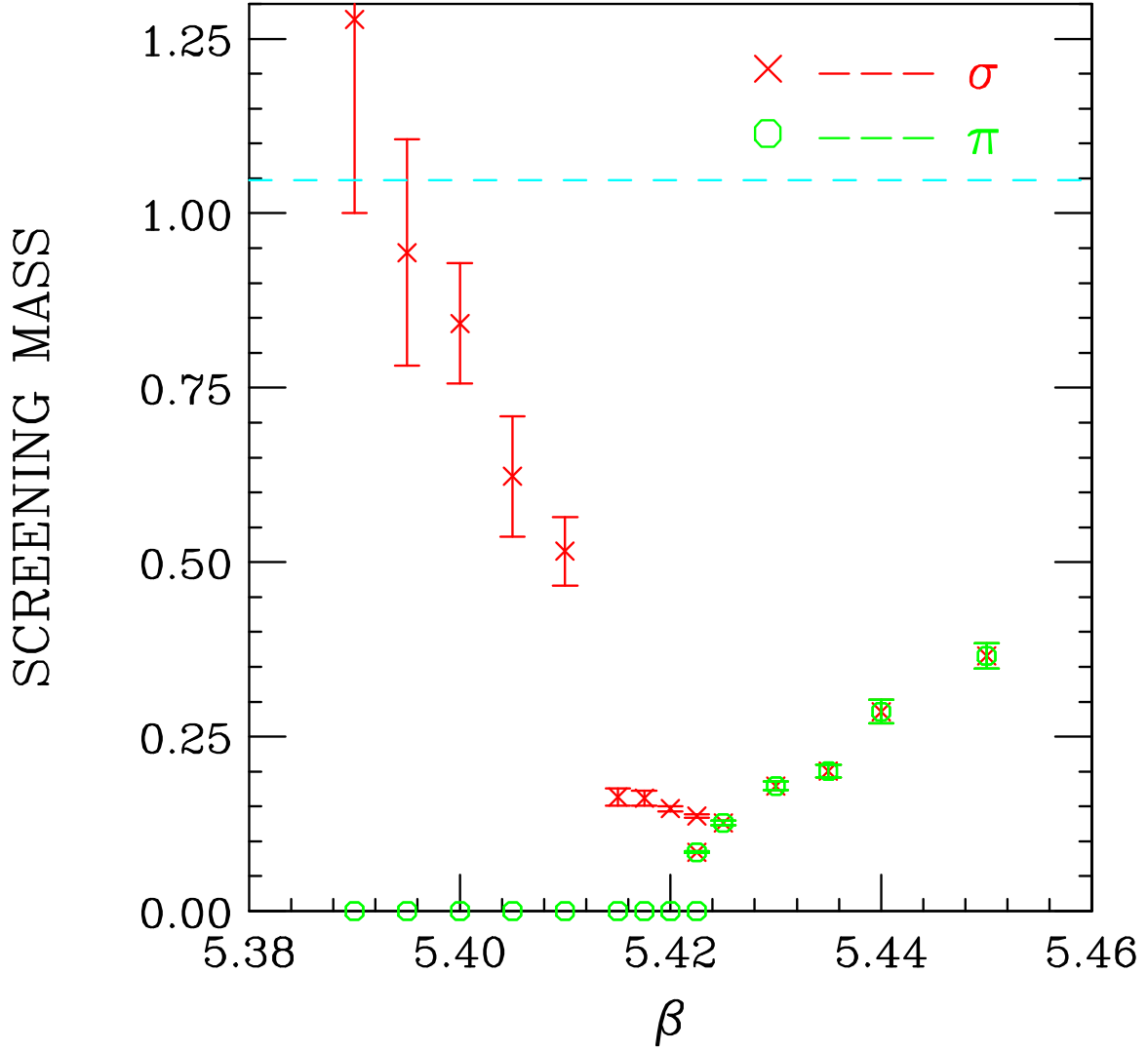


FIG. 4. σ and π screening masses as functions of β . Note that we have forced the pion mass to be zero below the transition and the σ and π masses to be equal above the transition. The dashed line is at $m=3$.

determined from our measurements. To 1-loop order the partial energy densities for the gluons and the quarks are given by [21]

$$\frac{s_g}{T^3} = \frac{4}{3} N_t^4 \frac{6}{g^2} \left(1 + g^2 \frac{1}{2} \frac{\partial C}{\partial g} \right) \left[\frac{\partial C}{\partial g} \right]_{[P_{ss}] [P_{st}]} \quad (24)$$

and

$$\frac{s_f}{T^3} = \frac{4}{3} N_t^4 \left(1 + g^2 \frac{\partial C_F}{\partial g} \right) \frac{N_f}{4} \left(\frac{3}{4} \right)$$

$$+ \frac{1}{2} \left(1 + \frac{g^2}{2} + 4g^2 \frac{C_m}{a} \right) \frac{N_f}{8} h^2 + \dots \quad (25)$$

where P_{ss} and P_{st} are the space-space and space-time plaquettes respectively. The coefficient functions are given in reference [21]. Since such expansions in terms of lattice couplings are notoriously poor, and an improved staggered fermion lattice perturbation expansion [22] for these quantities has yet to be performed, we present graphs of the tree level as well as the 1-loop results for these quantities in figures 5, 6. The Stephan-Boltzmann value for $s_{g(\text{ue})}=T^3$ is $32^{-2}=45 = 7.0184$. The finite lattice size/spacing effects on an $18^3 \times 6$ lattice increase this to 8.0951. The Stephan-Boltzmann value for $s_{f(\text{em})}=T^3$ is $7^{-2}N_f=15 = 9.2116$ which becomes 16.9823 on an $18^3 \times 6$ lattice. We note that both partial entropies increase rapidly from rather small values near the critical point and flatten out as the system passes into the plasma phase. The gauge field partial entropy lies above the Stephan-Boltzmann value in the plasma region, while the quark field partial entropy is about half its Stephan-Boltzmann limit. However, it should be noted that, since the β -screening masses indicate that the quarks in these mesonic excitations are still deeply bound at these values, the high temperature limit would not be expected until a considerably higher β .

In addition to these zero mass simulations, we have performed simulations at finite mass on a $12^3 \times 6$ lattice. For these simulations we fixed $\beta = \beta_c$. Here, the presence of even a relatively small symmetry breaking mass term was sufficient to align the condensate in the direction of h_1 (or h_2) so that we were able to measure the chiral condensate directly. The chiral condensate at $\beta = 10$ as a function of quark mass is given in table V, while that for $\beta = 20$ is given in table VI.

V. CRITICAL SCALING

Much of what is presented here was presented in our letter [10]. We repeat these results here for completeness, along with results which have not been presented before.

18³×6 LATTICE $\gamma=20$

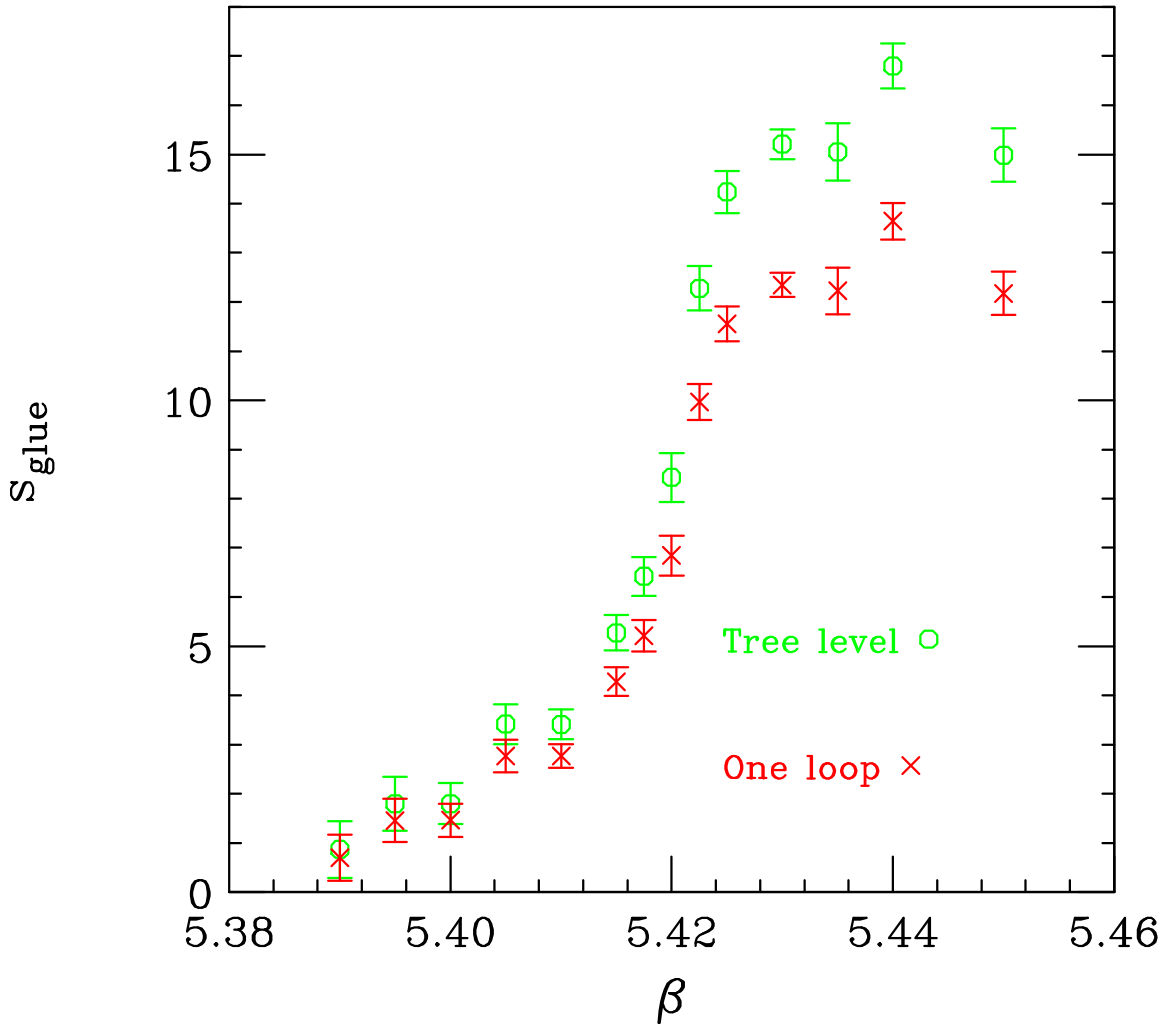


FIG. 5. Gluon partial energy density as a function of

Fitting the measured values of S_{glue} on a $18^3 \times 6$ lattice given in table I to the scaling form $S_{\text{glue}} = C (\beta - \beta_c)^{m_{\text{ag}}}$ for the interval $5.41 < \beta < 5.4225$ yields $\beta_c = 5.4230(2)$, $C = 1.19(12)$ and $m_{\text{ag}} = 0.27(2)$ with a 94% confidence level. On a $12^3 \times 6$ lattice, also at $\gamma = 20$, fits to the values in table III gave $\beta_c = 5.4249(7)$, $C = 1.46(22)$ and $m_{\text{ag}} = 0.32(4)$ at a 27% confidence interval. Our $12^3 \times 6$ measurements at $\beta = 10$ (table IV) yielded $\beta_c = 5.4650(1)$ and $m_{\text{ag}} = 0.27(3)$.

Clearly the sizable finite volume effects in these measurements are a major source of systematic errors. Having two different size lattices at $\beta = 10$ enables us to remove the

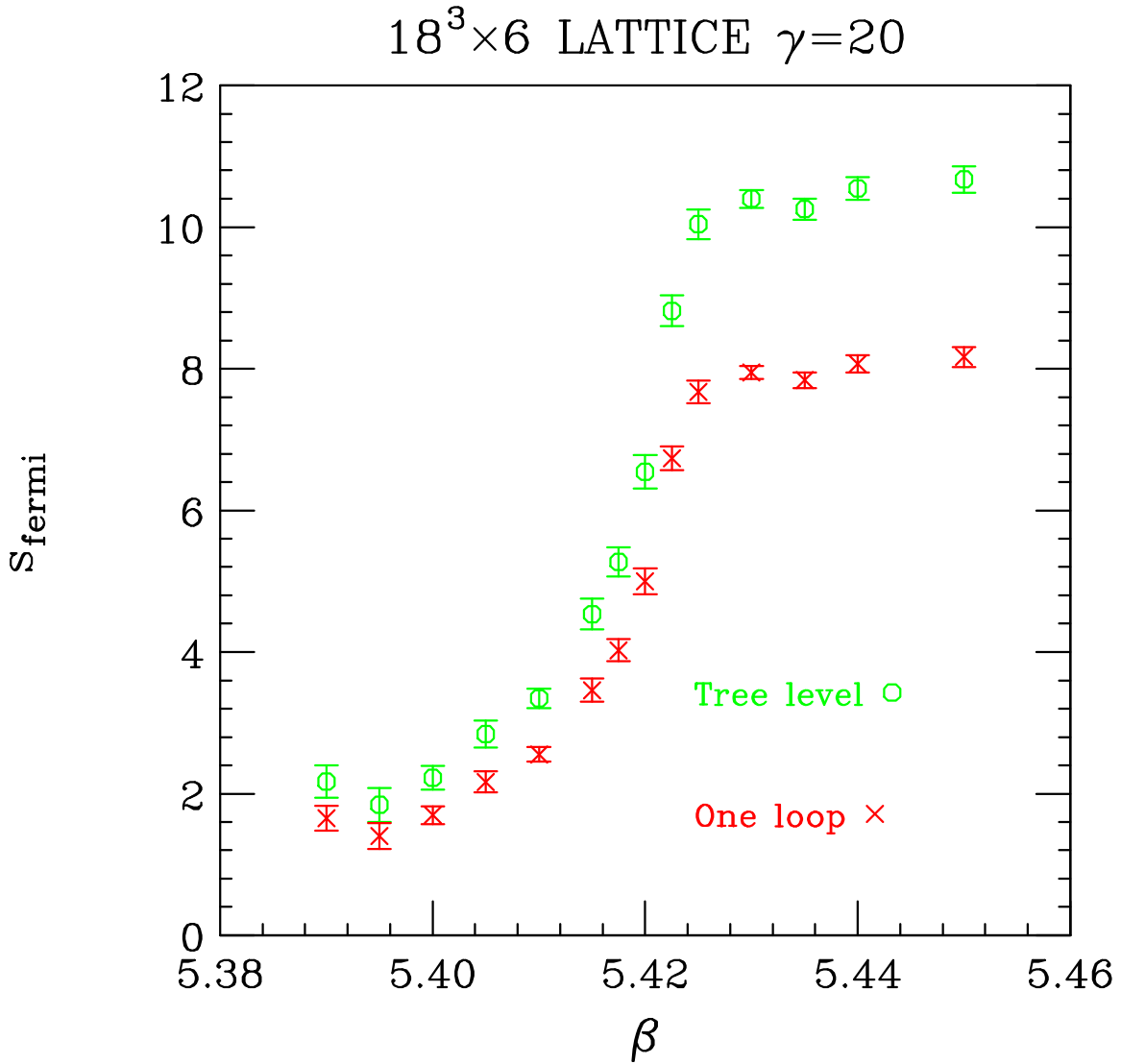


FIG. 6. Quark partial energy density as a function of

leading order finite volume effects. Here we note that

$$\langle \bar{\psi} \psi \rangle^2 = \langle \bar{\psi} \psi \rangle_{5,5} \langle \bar{\psi} \psi \rangle_{1^3} + \text{constant} = V \quad (26)$$

where here the inner $\langle \bar{\psi} \psi \rangle$ stands for averaging over the lattice and the outer $\langle \bar{\psi} \psi \rangle$ stands for the ensemble average. Table V II gives this quantity for the $12^3 \times 6$ lattice, the $18^3 \times 6$ lattice and the extrapolation to an $1^3 \times 6$ lattice where it gives us an estimate of $\langle \bar{\psi} \psi \rangle_{1^3}$. Fitting this estimate of $\langle \bar{\psi} \psi \rangle$ to the scaling form over the range $5.41 < \beta < 5.4225$, used for the lattices of finite spatial volume gives $\beta_c = 5.42270(15)$, $C = 1.06(11)$, $\beta_{\text{mag}} = 0.24(2)$ at a 78% confidence level. However, it is possible to fit this extrapolated chiral condensate

$\beta = 10, \quad \beta_c = 5.465$		
	h_i	Time'
0.004	0.397 (3)	20000
0.005	0.427 (3)	25000
0.006	0.446 (2)	25000
0.007	0.461 (2)	25000
0.010	0.512 (2)	5000
0.015	0.561 (1)	20000
0.020	0.606 (2)	5000
0.030	0.674 (2)	5000

TABLE V. Mass dependence of h_i at β_c for $\beta = 10$.

$\beta = 20, \quad \beta_c = 5.23$		
	h_i	Time'
0.0030	0.256 (6)	10000
0.0040	0.329 (4)	10000
0.0050	0.331 (4)	10000
0.0075	0.387 (2)	10000
0.0100	0.421 (2)	15000
0.0150	0.478 (1)	15000
0.0200	0.534 (3)	3000
0.0300	0.594 (2)	3000

TABLE VI. Mass dependence of h_i at β_c for $\beta = 20$.

over the complete range $5.39 < \beta < 5.4225$, yielding $\beta_c = 5.42267(10)$, $C = 1.00(3)$ and $m_{ag} = 0.229(9)$ while the confidence level only drops to 60%. The plot of this estimate of the chiral condensate with this latter fit superimposed is given in figure 7. Finally we note that if one fixes $m_{ag} = \frac{1}{4}$, its tricritical value, one obtains a fit with confidence level 89% over

	$12^3 \times 6$	$18^3 \times 6$	$1^3 \times 6$
5.39000	0.231 (2)	0.2150 (17)	0.2083 (25)
5.39500	0.200 (2)	0.1970 (29)	0.1957 (41)
5.40000	0.184 (2)	0.1760 (19)	0.1726 (28)
5.40500	0.179 (2)	0.1601 (27)	0.1521 (39)
5.41000	0.145 (1)	0.1393 (16)	0.1370 (24)
5.41500	0.120 (2)	0.1091 (32)	0.1045 (47)
5.41750	0.0961 (4)	0.0920 (36)	0.0902 (51)
5.42000	0.0731 (4)	0.0678 (38)	0.0656 (54)
5.42125	0.0796 (2)		
5.42250	0.0610 (1)	0.0311 (32)	0.0184 (45)
5.42500	0.0531 (5)	0.0133 (22)	-0.0035 (32)
5.43000	0.0243 (2)	0.00608 (62)	-0.0016 (9)
5.43500		0.00396 (41)	
5.44000		0.00255 (17)	
5.45000		0.00160 (7)	

TABLE VII. Averages of squares of the chiral condensate on $12^3 \times 6$ and $18^3 \times 6$ lattices and the extrapolation to infinite spatial volume.

the range 5.41 – 5.4225, which falls to 20% over the complete range 5.39 – 5.4225. From all these fits we conclude that the value of m_{ag} is consistent with that of the 3-dimensional tricritical point, but inconsistent with either the O(4) or O(2) values.

We now turn to consideration of the scaling of h with quark mass m at $\beta = \beta_c$. This is difficult to perform with the usual staggered formulation, since it is hard to determine β_c with sufficient precision. In addition, for m small enough, h vanishes linearly with m on a configuration by configuration basis at any β . In our formulation, not only can β_c

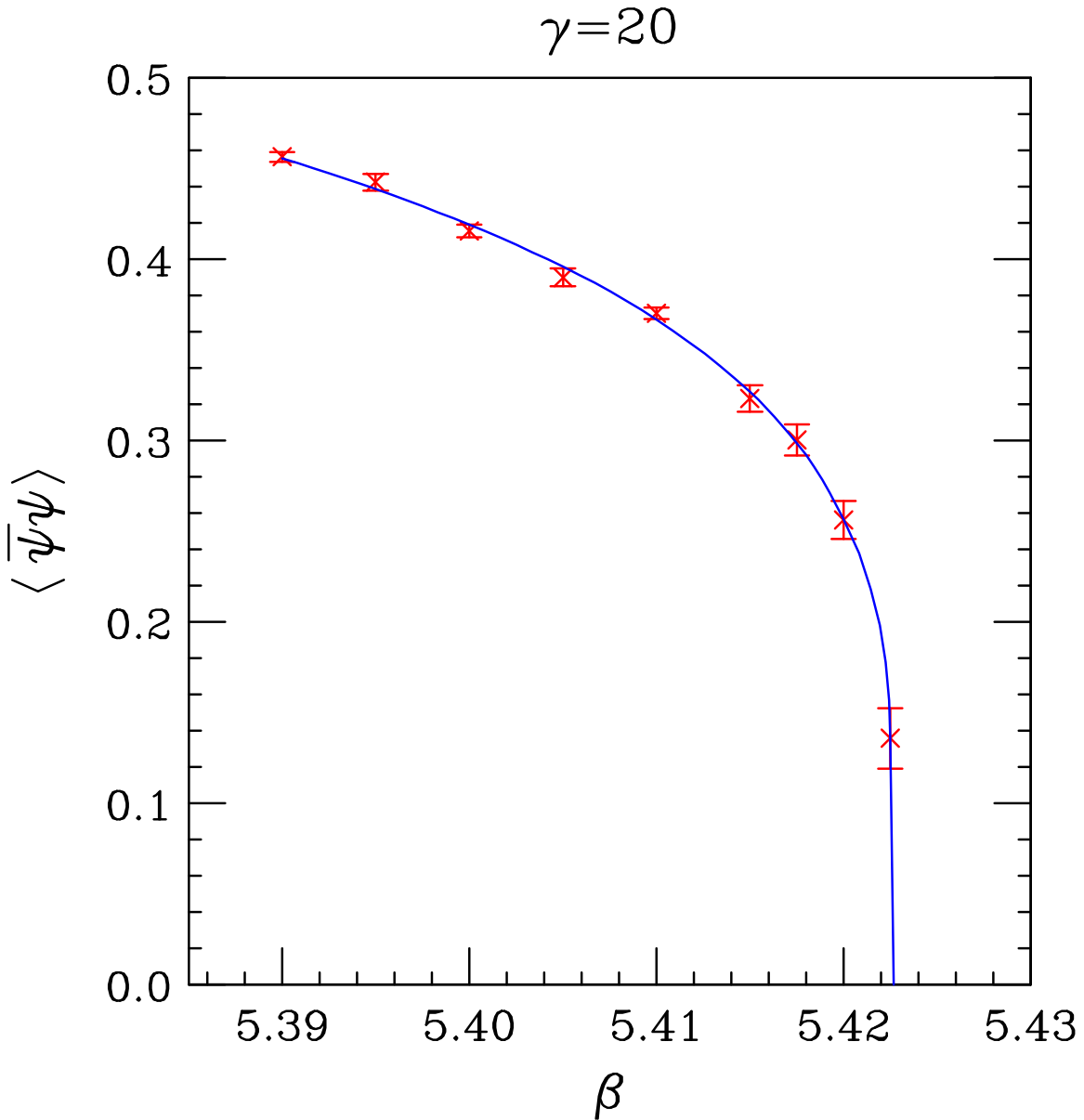


FIG. 7. $\langle \bar{\psi}\psi \rangle$ versus β with critical scaling curve superimposed.

be determined with adequate precision, but the chiral condensate remains finite on each configuration as $m \rightarrow 0$ for $\beta < \beta_c$ and presumably should vanish as the appropriate power ($l=$) of m at $\beta = \beta_c$. What a finite mass does is orient the condensate in the required direction. The value of m required to achieve such orientation should be somewhat smaller than that required to avoid the region of linear vanishing in the conventional approach. We fitted the $12^3 \times 6$, $\gamma = 10$ results of table V to the scaling form $\langle \bar{\psi}\psi \rangle = D m^{1-l}$. Our best fit gives $D = 1.66(2)$ and $\beta_c = 3.89(3)$. This fit has only a 4% confidence level. However,

removing the point at $m = 0.01$ which lies 2.5 standard deviations from the curve increases the confidence level to 33% with negligible change to D and β . We note that this value is incompatible with the $O(4)$ or $O(2)$ values. It does, however, lie between the two values (3 and 5) for the 3-dimensional tricritical point. The more general scaling can be obtained starting with the ϕ^6 effective field theory which describes tricritical behaviour. As argued in section 2, this can be treated in mean field approximation since it is at the upper critical dimension. The effective Hamiltonian for this theory is

$$H = \frac{1}{6} \phi^6 - m \frac{1}{5} \phi^5 + u \frac{1}{4} \phi^4 - m \frac{1}{3} \phi^3 + t \frac{1}{2} \phi^2 + \text{const} \quad (27)$$

The odd powers of ϕ are the symmetry breaking terms. Hence we identify them with the m and t terms in our Lagrangian, i.e.

$$h = a + b \frac{1}{3} \phi^3 + c \frac{1}{5} \phi^5 \quad (28)$$

Note here that we have kept the third symmetry breaking operator ϕ^5 which has $\beta = 1$, since we do not have the luxury of redefining ϕ to remove it. Since we are considering the case where we are at the tricritical point for $m = 0$, the 2 reduced temperatures u and t are also zero. The vacuum expectation value of ϕ is that which minimizes H . Thus ϕ is the real positive solution of

$$5m(a + b\phi^2 + c\phi^4) = 0 \quad (29)$$

Thus we substitute into the form of equation 28 with ϕ given in equation 29. We obtained a fit with $a = 1.05(2)$, $b = 2.5(4)$, $c = 3.1(1.4)$. Although this fit had only a 2% confidence level, removing the point at $m = 0.01$ gives a fit with parameters consistent with those including this point, but with a 35% confidence level. In fact, it is easy to convince oneself that any reasonably smooth fit would have difficulty fitting this point. We have plotted the measurements of table V in figure 8 with this fit superimposed. Estimates of the errors induced in these measurements by the error in determining ϕ_c have been made from the tricritical scaling function, f_{QCD} and found to be small.

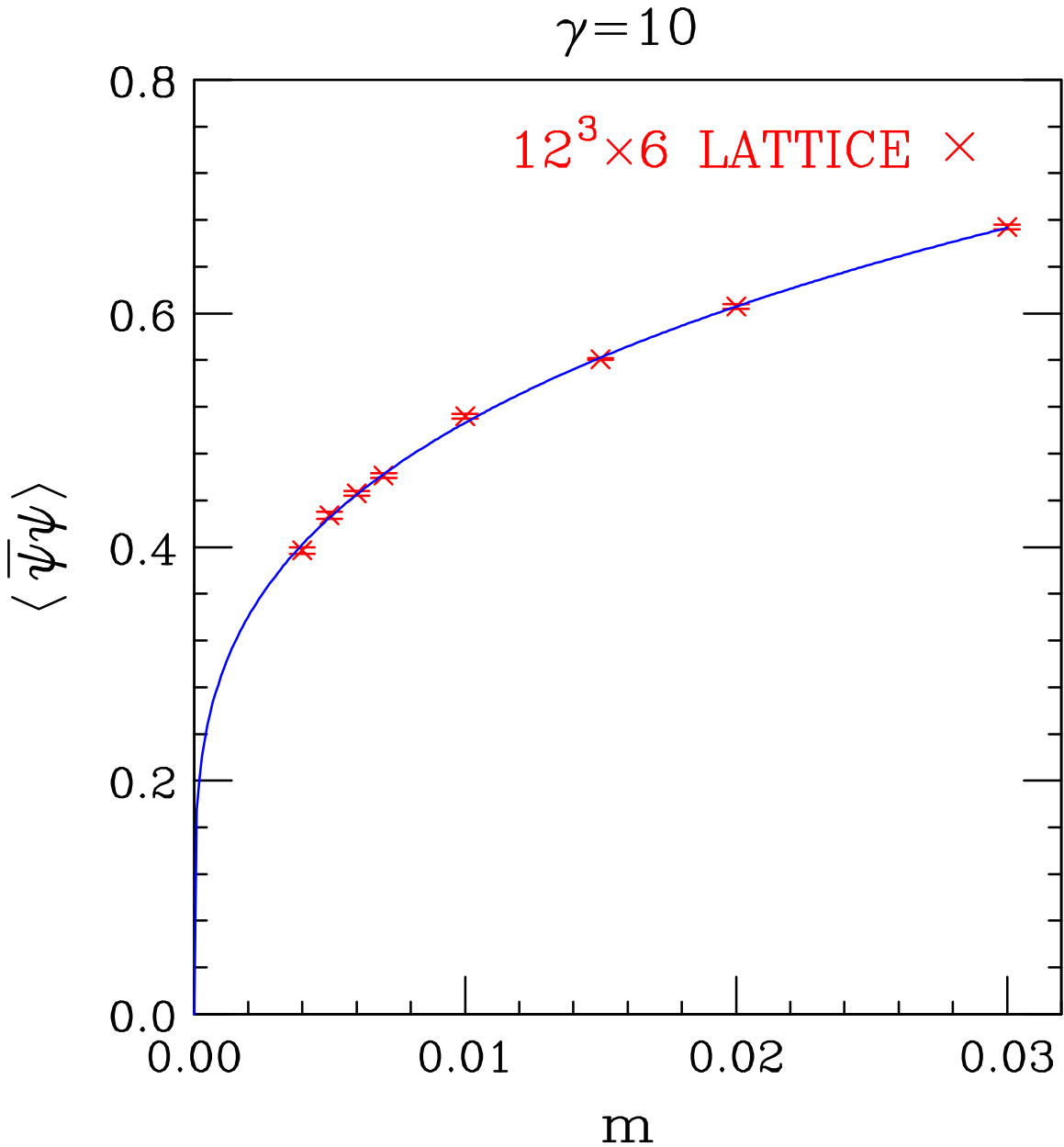


FIG .8. M ass dependence of $\langle \bar{\psi}\psi \rangle$ at $\gamma = 10$.

Our measurements of the mass dependence of $\langle \bar{\psi}\psi \rangle$ on a $12^3 \times 6$ lattice at $\gamma = 20$ given in table VI are somewhat poorer than those at $\gamma = 10$. For this reason we are unable to get reasonable fits to this 'data'. To clarify this, we have plotted this 'data' in figure 9. Just looking at the points, we notice that the $m = 0.004$ and $m = 0.005$ points are clearly incompatible. After several trials we found it that the $m = 0.005$ point should be excluded. Smoothness criteria caused us to also exclude the $m = 0.02$ point. Even then no

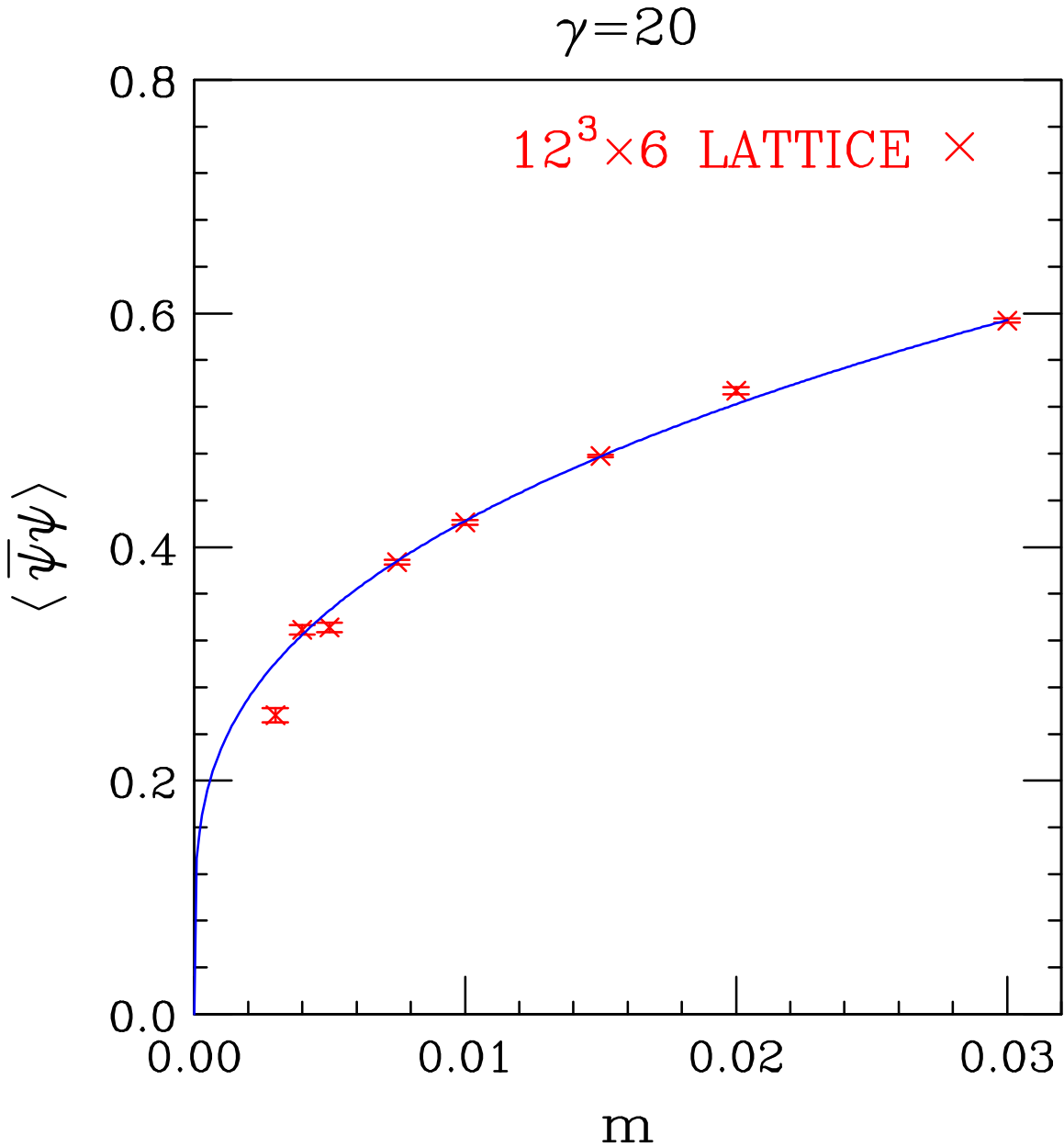


FIG. 9. Mass dependence of $\langle \bar{\psi} \psi \rangle$ at c_c for $\gamma = 20$.

it came close to the $m = 0.003$ point. Here we suspect that this is because c_c was more poorly determined than in the $\gamma = 10$ case. Deviations of c_c from c_c have the most effect on the lowest mass point as is clear from equation 9. Excluding these 3 points allows a fit with $a = 0.83(3)$, $b = 3.2(5)$, $c = 2.5(1.5)$ at a 38% confidence level. This curve is plotted in figure 9. Clearly such a fit should be considered at best suggestive, so we base our conclusion that the scaling of $\langle \bar{\psi} \psi \rangle$ with mass is in accord with tricritical scaling purely on the $\gamma = 10$

measurements.

From the plot of screening masses of figure 4, it is clear that nothing quantitative can be obtained from the masses in the low temperature domain. We have therefore concentrated our efforts on fitting the joint β -screening masses in the plasma region to the scaling form $m_s = A(\beta - \beta_c)$. Since different treatment of these screening masses in the hadronic matter and quark-gluon plasma phases could bias our results, we chose to adopt the joint fit of the β and β propagators of equation 23 over the whole range of β . This fit will be correct in the plasma phase. In the low temperature phase, the non-zero vacuum expectation value of the β field should drive the fitted mass to zero. Fitting these screening masses to the screening form for $\beta > \beta_c$ (in fact we use all points for which $\beta > 5.4225$) we find $A = 2.66(71)$, $\beta_c = 5.4196(7)$ and $\nu = 0.59(7)$ admittedly with only a 0.3% confidence level. Plotting this fit on a graph figure 10 of mass measurements, it is clear why: the point at $\beta = 5.35$ is clearly inconsistent with those at $\beta = 5.44$ and $\beta = 5.45$. Removing the point at $\beta = 5.35$ improves the confidence level to an acceptable 39% while only changing the fitting parameters within errors (for example $\nu = 0.62(6)$). We attribute this to the systematic errors in performing fits to point-source propagators with a lattice extent of only 18 and limited statistics. From these fits we conclude that ν is consistent with the tricritical value ($\frac{1}{2}$), but does not rule out an O(4) or O(2) value.

We have extracted a susceptibility from our 'data' on the $18^3 \times 6$ lattice at $\beta = 20$ using $\chi = V [\langle h^2 \rangle - \langle h \rangle^2]$. Since our estimate of $\langle h \rangle$ was obtained after rotating h to where $\langle h \rangle = 0$ configuration by configuration this actually defines a 'radial' rather than the conventional susceptibility. However, this should diverge in the same manner as the conventional susceptibility, which is all that matters. Fitting to the form $\chi = c_j (\beta - \beta_c)^{\nu_{mag}}$ over the range $5.405 < \beta < 5.45$ gives $\beta_c = 5.4215(1)$, $c = 0.0096(11)$ and $\nu_{mag} = 0.66(3)$ with a 31% confidence level. Our measurements and fit are plotted in figure 11. Since the value of this critical exponent lies between the ν_{mag} values ($\frac{1}{2}$ and 1) associated with the tricritical point, but far from the O(4) and O(2) exponents this is further evidence for

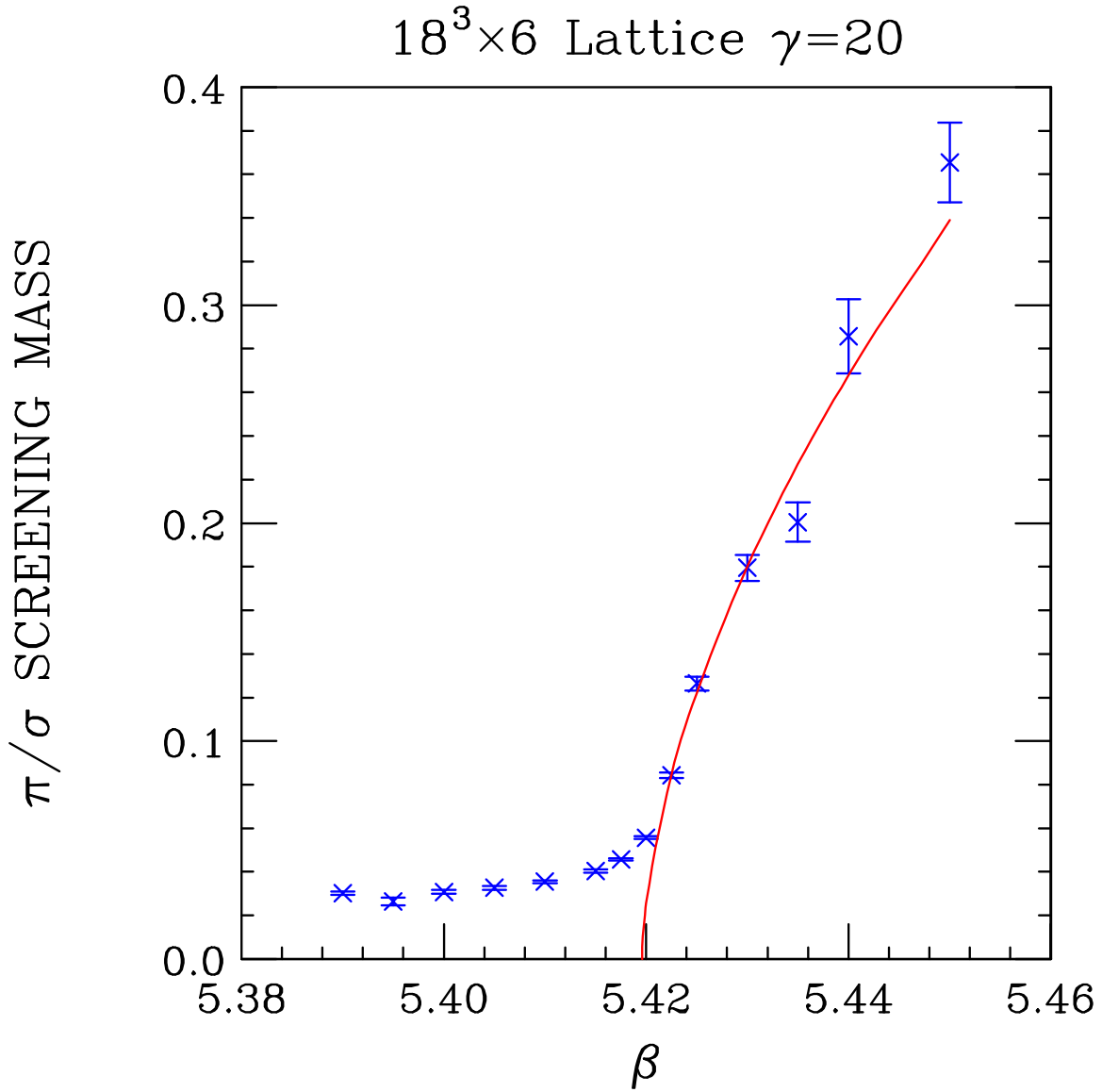


FIG .10. Joint / screening masses as functions of β .

tricriticality. The reason we did not use the h₁ susceptibility is that our measurements of h₁ are noisy estimators using a single noise vector per configuration which gives extra contributions to the susceptibility estimate that can only be removed by use of more than one noise vector per configuration.

$18^3 \times 6$ LATTICE

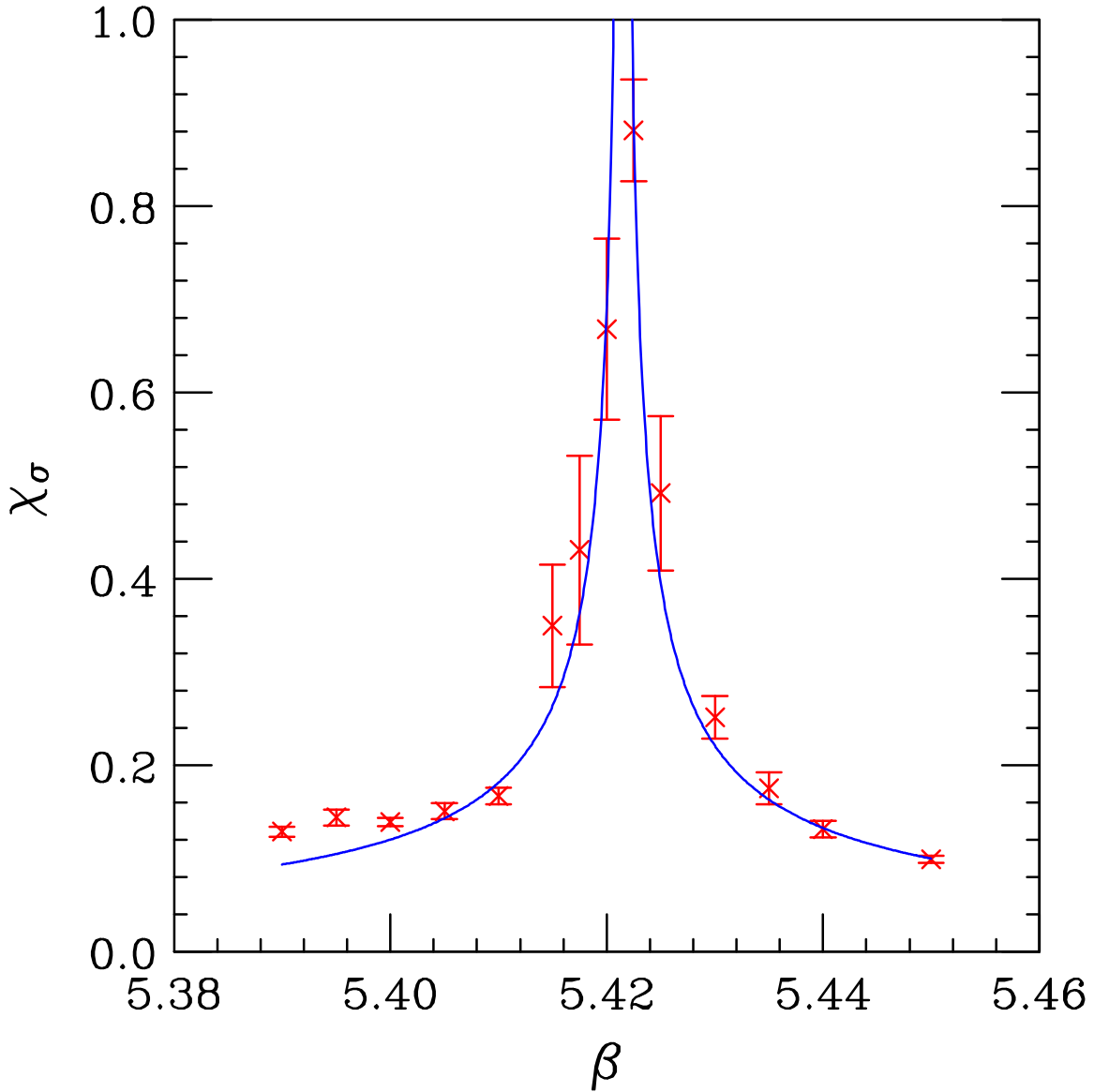


FIG .11. susceptibility as a function of β .

VI. DISCUSSION AND CONCLUSIONS

We have presented evidence that the $N_t = 6$ finite temperature phase transition for 2-avour staggered lattice QCD with extra chiral 4-fermion interactions is in the universality class of a 3-dimensional tricritical point rather than that of the 3-dimensional $O(4)$ or $O(2)$ sigma model, which was expected. Since a tricritical point occurs when there are extra

relevant operators with consequent competing transitions, we believe this to be due to the extra higher-dimensional operators which can be important on such coarse lattices. For this reason, we believe the $O(4)/O(2)$ universality class would be observed for sufficiently fine lattices, i.e. those with sufficiently large N_t . Since the $N_t = 4$ transition with $\beta = 10$ was observed to be first order, and a tricritical point marks the transition from first order to universal second order behaviour, this strongly suggests that $O(4)/O(2)$ universality would be observed for N_t as small as 8.

The fact that our modified action allowed us to work at zero quark mass was crucial in allowing us to come to these conclusions. This enabled us to measure the critical exponent ν_{mag} directly. Our best estimates lay in the range $0.23 < \nu_{\text{mag}} < 0.27$ (with errors typically around 2 in the second decimal place) which is consistent with the $\frac{1}{4}$ of the tricritical point, but inconsistent with the 0.384(5) of the $O(4)$ sigma model, the 0.35(1) of the $O(2)$ sigma model and the $\frac{1}{2}$ of mean field theory. Because these scaling fits give precise estimates for ν_c , it is possible to measure ν_{mag} directly from the scaling of the chiral condensate with quark mass with β fixed at β_c . This value, $\nu_{\text{mag}} = 3.89(3)$, lay between the two values (3 and 5) of the tricritical point, and a satisfactory fit to the more complex scaling this implies was obtained. Again this behaviour was incompatible with $O(4)/O(2)$ scaling where $\nu_{\text{mag}} = 4/3$ and mean field scaling with $\nu_{\text{mag}} = 3$. The scaling of the χ mass in the plasma domain yielded a value which was compatible with tricritical, $O(4)/O(2)$ and mean field scaling. Finally we were able to extract the susceptibility critical exponent $\nu_{\text{mag}} = 0.66(3)$ which lies between the two values ($\frac{1}{2}$ and 1) of the tricritical point but disagrees with the $O(4)/O(2)$ values (1.328(6) and 1.471(6)) and the mean field value (1).

Since we believe we are seeing more complex phase structure which is driven by lattice artifacts, the behaviour we are seeing does not have to apply to the standard staggered action. However, since scaling analyses with the standard action on $N_t = 4$ lattices showed definite departures from $O(4)/O(2)$ universality [5,6,8,9] it strongly suggests that some such behaviour is present. In fact, based on our earlier, $N_t = 4$ results one of the collaborations

suggested [8] that these anomalies might be associated with the first order transition we reported in [2]. Unfortunately there are not yet sufficient high precision measurements with the standard action at $N_t = 6$ to tell if it too displays departures from $O(4)/O(2)$ universality.

Clearly, simulations at $N_t = 8$ should be next on our agenda. We would also suggest that the addition of such 4-fermion terms should be considered for other actions, especially improved staggered actions.

ACKNOWLEDGEMENTS

These computations were performed on the CRAY C90/J90/SV1's and T3E at NERSC, and on a T3E at SGI/Cray. We thank J.F. Lagae who contributed to the earlier stages of this work. We would also like to thank M. Stephanov for educating us on tricritical behaviour. Finally we wish to thank C. DeTar for providing us with the $O(4)$ scaling functions used by the MILC collaboration. This work was supported by the U.S. Department of Energy under contract W-31-109-ENG-38 and the National Science Foundation grant NSF-PHY 96-05199.

REFERENCES

- [1] S. Duane and J. B. Kogut, *Phys. Rev. Lett.* 55, 2774 (1985); S. Gottlieb, W. Liu, D. Toussaint, R. L. Renken and R. L. Sugar, *Phys. Rev. D* 35, 2531 (1987); S. Duane, A. D. Kennedy, B. J. Pendelton and D. Roweth, *Phys. Lett. B* 195, 216 (1987).
- [2] J.-F. Lagae, J. B. Kogut and D. K. Sinclair, *Phys. Rev. D* 58, 34004 (1998).
- [3] J. Smith and J. C. Vink, *Nucl. Phys. B* 286, 485 (1987).
- [4] F. Karsch, *Phys. Rev. D* 49, 3791 (1994); F. Karsch and E. Laermann, *Phys. Rev. D* 50, 6954 (1994).
- [5] S. Aoki, et al. (JLQCD Collaboration), *Phys. Rev. D* 57, 3910 (1998).
- [6] G. Boyd with F. Karsch, E. Laermann and M. Oevers, *Proceedings of 10th International Conference Problems of Quantum Field Theory, Alushta, Crimea, Ukraine* (1996).
- [7] D. Toussaint, *Phys. Rev. D* 55, 362 (1997).
- [8] C. Bernard et al. (MILC collaboration) *Nucl. Phys. B (Proc. Suppl.)* 63A-C, 400 (1998); *Phys. Rev. D* 61, 054503 (2000).
- [9] E. Laermann, *Nucl. Phys. B (Proc. Suppl.)* 63A-C, 114 (1998).
- [10] J. B. Kogut and D. K. Sinclair, *Phys. Lett. B* 492, 228 (2000).
- [11] K. I. Kondo, H. Mino and K. Yamawaki, *Phys. Rev. D* 39, 2430 (1989).
- [12] R. C. Brower, Y. Shen and C.-I. Tan, Boston University preprint BUHEP-94-3 (1994); R. C. Brower, K. Orginos and C.-I. Tan, *Nucl. Phys. B (Proc. Suppl.)*, 42 (1995).
- [13] S. Hands, A. Kocic and J. B. Kogut, *Ann. Phys.* 224 (1993).
- [14] S. Kim, A. Kocic and J. B. Kogut, *Nucl. Phys. B* 429, 407 (1994)
- [15] S. Hands, A. Kocic and J. B. Kogut, e-print hep-lat/9705038 (1997).

- [16] D. J. Amit, *Field Theory, the Renormalization Group, and Critical Phenomena* (McGraw-Hill, New York, 1978).
- [17] J. I. Kapusta, *Finite Temperature Field Theory* (Cambridge University Press, 1989).
- [18] R. Pisarski and F. Wilczek, *Phys. Rev. D* 29, 338 (1984).
- [19] G. Baker, D. Merion and B. Nickel, *Phys. Rev. B* 17, 1365 (1978); J. C. Le Guillou and J. Zinn-Justin, *Phys. Rev. B* 21, 3976 (1980); K. Kanaya and S. Kaya, *Phys. Rev. D* 51, 2404 (1995); P. Butera and M. Comi, *Phys. Rev. B* 52, 6185 (1995).
- [20] I. D. Lawrie and S. Sarbach, in *Phase Transitions and Critical Phenomena, Volume 9* (Academic Press, London, 1984).
- [21] M. Chavel, *Phys. Rev. D* 58, 074503 (1998).
- [22] M. Goltermann, *Nucl. Phys. B (Proc. Suppl.)* 73, 906 (1999).